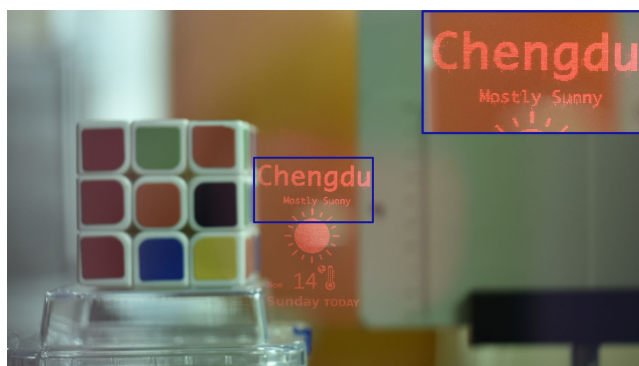


Generation of Phase-Only Holograms Based on Aliasing Reuse and Application in Holographic See-Through Display System

Volume 11, Number 3, June 2019

Chun Chen
Min-Yang He
Jun Wang
Ke-Ming Chang
Qiong-Hua Wang



DOI: 10.1109/JPHOT.2019.2911981
1943-0655 © 2019 IEEE

Generation of Phase-Only Holograms Based on Aliasing Reuse and Application in Holographic See-Through Display System

Chun Chen,¹ Min-Yang He,¹ Jun Wang ¹, Ke-Ming Chang,¹
and Qiong-Hua Wang ²

¹School of Electronics and Information Engineering, Sichuan University, Chengdu 610065, China

²School of Instrumentation and Optoelectronic Engineering, Beihang University, Beijing 100191, China

DOI:10.1109/JPHOT.2019.2911981

1943-0655 © 2019 IEEE. Translations and content mining are permitted for academic research only. Personal use is also permitted, but republication/redistribution requires IEEE permission. See http://www.ieee.org/publications_standards/publications/rights/index.html for more information.

Manuscript received February 21, 2019; revised April 4, 2019; accepted April 15, 2019. Date of publication April 18, 2019; date of current version May 14, 2019. This work was supported in part by the National Key Research and Development Program of China (2017YFB1002900) and in part by Sichuan Science and Technology Program (2018GZ0533). Corresponding author: Jun Wang (e-mail: jwang@scu.edu.cn).

This paper has supplementary downloadable material available at <http://ieeexplore.ieee.org>, provided by the authors.

Abstract: In the point-based method, the aliasing phenomenon in the hologram plane is usually considered as a harmful phenomenon because it will degrade the reconstructed image quality. In this paper, the advantage of the aliasing phenomenon is employed to improve the reconstructed image quality of the phase-only hologram. Through analysis of the principle of this phenomenon, we proposed a method to improve the reconstructed image quality of the phase-only hologram. By controlling the strength of the aliasing, the amplitude distribution in the hologram plane can be turned into a nearly uniform distribution. It is helpful to generate an optimized phase-only hologram, which results in higher quality of the reconstructed image because the effect of lost information caused by abandon the amplitude part can be diminished. Moreover, a holographic see-through display system is designed to demonstrate the effectiveness of the proposed method.

Index Terms: Computer holography, holographic display, augmented reality.

1. Introduction

Augmented reality (AR) technology can mix visual signal into real-world scenes, which allow the user to see both real scenes and visual signals at the same time. This new technology gives us a chance to observing the world from a different perspective and can be applied in various fields, such as navigation, medicine, entertainment, and national defense [1]–[3]. Among the existing AR systems, the see-through head-mounted display plays an essential role. However, in the traditional see-through head-mounted display, one of the issues is the accommodation-vergence conflict problem, which will cause some side effects to the viewer (eye fatigue, eye irritation, headache, etc) [4]–[8]. Holography is regarded as a promise technology for 3D display, which is able to provide all the information observers need, therefore, it's pretty suited for AR display system [9]–[12].

In holography display, one of the major problems of the holography for dynamic 3D display is the calculation speed of computer-generated holograms (CGHs), many methods have been proposed to solve the problem [13], [14]. The look-up table (LUT) method [15]–[19] considers that the point light source consists of the object, and all of the point fringe patterns are pre-calculated. Since the hologram can be calculated by adding together all the fringe patterns, the calculation speed can be dramatically improved. Another problem of holography display is the degradation of the reconstructed image quality because of the phase or amplitude information is lost. By adding an initial random phase to the object, the phase-only hologram can preserve most amplitude information of the object [20]. Nevertheless, the speckle noise is appeared in the reconstructed image due to the interference among points, which reduces the image quality. Therefore, many methods have been proposed to improve the image quality in phase-only hologram reconstruction, such as the iterative CGH algorithm [21], [22], time-integrating method [23], [24], multi-random phase method [25], error diffusion method [26], [27] and down-sampling method [28]. However, there are still some problems, which include a long calculation time and the need for a spatial light modulator (SLM) with a high frame rate. The limitations of those methods will influence its application for the dynamic and high-quality AR display. The aliasing phenomenon is considered as another factor which can degrade the image quality [29]. In the point-based model, the aliasing phenomenon usually appears in the hologram plane and degrades the reconstructed image quality, which will cause the overlapped phenomenon when in defocus reconstruction [30]–[32]. However, further analysis of it has not yet be explained explicitly. The aliasing phenomenon usually is considered as harmful to the holographic display, while this phenomenon will not consume additional calculation time. Whether it is possible that the aliasing could be used to improve the holographic display quality is worth discussing.

In this paper, we analyze the reason of the aliasing phenomenon in the point-based model and propose a novel and simple method to improve the reconstructed image quality in phase-only hologram by taking the advantage of this phenomenon. Through change the sampling interval of the object, we can control the strength of the aliasing in the hologram plane. With the proposed method, the diffraction field in the hologram plane will be overlapped, and the amplitude distribution of it will become a nearly uniform distribution, which diminishes the effect of lost amplitude information. Additionally, the overlapped phenomenon in reconstructed image can be replaced by the defocus blur phenomenon, and the larger sampling interval will suppress the speckle noise in the reconstructed image. Therefore, the reconstructed image quality can be improved with the proposed method. Moreover, we designed a holographic see-through display system to demonstrate the effectiveness of the proposed method in high-quality AR display.

2. Point-Based Model

In the point-based method, a 3D object can be considered as a collection of self-luminous points of light, each point has a wavefront in the hologram plane. Assume the object point and the hologram plane position are at (x_i, y_i, z_i) and $z = 0$, respectively. And each point is assumed to have an associated amplitude and phase of a_i, φ_i . Then, the complex amplitude $U(x, y)$ in the hologram plane can be obtained by superposing all of the wavefronts, as expressed by Eq. (1):

$$U(x, y) = \sum_{i=1}^{N_A} E(x, y) \frac{a_i}{r_i} \exp[j(kr_i + \varphi_i)], \quad (1)$$

where $k = 2\pi/\lambda$ is the wave number, λ is the wavelength of light and N_A represents the number of all points of the 3D object. $E(x, y)$ is an envelope function which is used to limit the region of contribution for a point light source. This function will limit the spatial frequency of the hologram fringe pattern to avoid the aliasing in the reconstructed image, in other words, this function will limit the divergence angle of the point light source [15]. r_i represents the distance between the object

point and the points $(x, y, 0)$ on the hologram plane, which is given by:

$$r_i = \sqrt{(x_i - x)^2 + (y_i - y)^2 + z_i^2}. \quad (2)$$

In Eq. (1), the computation complexity is high and the calculation is time-consuming. The LUT method can accelerate the calculation time by pre-calculated the fringe patterns and stored in memory, the expression of the fringe patterns is given as follow:

$$P_i(x_i, y_i, z_i) = \frac{\exp[j(kr_i + \varphi_i)]}{r_i}. \quad (3)$$

The wavefront $U(x, y)$ in the hologram plane can be obtained by add together all the fringe patterns and the phase-only hologram can be generated by removing the amplitude part of the wavefront $U(x, y)$. However, because of the amplitude distribution in the hologram is not uniformity, directly remove the amplitude part will lose the most information of the object. When the object is larger than the hologram plane, the larger part cannot recover from the hologram [33]. Adding random phase to the input image can solve the problems, but the method will cause the speckle noise problem in the reconstruction cause of the interference among points [34], [35]. In the following part, those problems should be solved by the proposed method.

3. Proposed Method Based on Aliasing Reuse

3.1 Principle

Except for the aliasing in the reconstructed image, there has another aliasing phenomenon which appears in the hologram plane. The proposed method takes advantage of the aliasing phenomenon to enhance the reconstructed image quality, and the principle of the proposed method is shown in Fig. 1. The resolution and sampling interval of the input object are $M_0 \times N_0$ and p_{x0}, p_{y0} , respectively. And the resolution and sampling interval of the enlarged object are $M_1 \times N_1$ and p_{x1}, p_{y1} , respectively. Firstly, we enlarge the sampling interval of the object to obtain larger physical size, the relations between the input object and the enlarged object are given by:

$$\begin{aligned} M_1 &= M_0, N_1 = N_0, \\ p_{x1} &= s \cdot p_{x0}, p_{y1} = t \cdot p_{y0}, \end{aligned} \quad (4)$$

where the s, t represent the scaling factors in x, y dimensions, respectively, and $s = t$. Secondly, the diffraction field in the hologram plane is calculated by using the point-based method. Thirdly, the phase-only hologram can be obtained by extract the phase component of the diffraction field. Here, this is not the only way to generate the phase-only hologram, we can also combine with other encoding methods such as double-phase method [36] to obtain the phase-only hologram. After the first two operations, the diffraction field of the object in the hologram plane will be duplicated in two-dimension and overlapped, which is also a kind of aliasing phenomenon. Fig. 2 shows the overlapped and duplicated diffraction field of the object in the hologram plane. In the previous studies [29]–[32], this phenomenon is considered as aliasing problem and will degrade the image quality. However, we also can take advantage of this phenomenon because it can be used to smooth the amplitude distribution in the hologram plane. In other words, this phenomenon will reduce the effect of lost amplitude information. In order to enhance the reconstructed image quality from the phase-only hologram, we need to control the number of the overlapped diffraction field in the hologram plane. There are three reasons to increase the number of it: (1) the overlapped diffraction field will turn the amplitude distribution into a nearly uniform distribution to decrease the effect of lost amplitude information in phase-only hologram, (2) the increased diffraction field in the hologram plane means the more information of the object can be recorded in hologram, (3) the overlapped diffraction field in the hologram plane will enhance the human visual quality of defocusing the reconstructed image since the blurring phenomenon replaced the overlapped phenomenon (detailed explain in Figs. 5(e) and 5(f)).

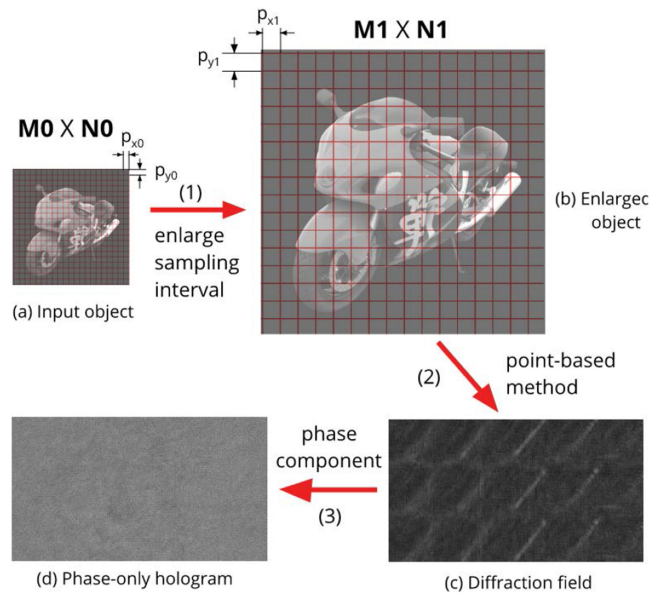


Fig. 1. The scheme of the proposed method.

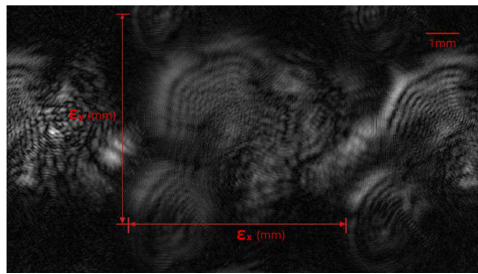


Fig. 2. Diffraction field in hologram plane with interval enlargement operation.

The number of the diffraction field is related to the wavelength, diffraction distance, and the object sampling interval. This phenomenon can be explained clearly by the principle of interference and the grating equation. We consider an object is composed of only two points, and these two points are at $z = d_1$ plane with interval $\Delta x_1 = p_{x1}$, $\Delta y_1 = 0$ in x, y dimension, respectively. The interference fringe interval ϵ in the hologram plane which is determined by:

$$\epsilon = d_1 \lambda / p_{x1}. \quad (5)$$

Although the object is composed of many points, the interval of the diffraction field in the hologram plane still can be approximately obtained by Eq. (4). According to Eq. (4), the intervals between two diffraction field in Fig. 2 are given by:

$$\begin{aligned} \epsilon_x &= d_1 \lambda / \Delta x_1, \\ \epsilon_y &= d_1 \lambda / \Delta y_1. \end{aligned} \quad (6)$$

The number of the diffraction field in hologram plane can be increased by enlarging the object sampling interval, and the numbers of the diffraction field in the x, y dimensional can be approximately

obtained by:

$$\begin{aligned} N_{dx} &= M \cdot \Delta x / \epsilon_x, \\ N_{dy} &= N \cdot \Delta y / \epsilon_y, \end{aligned} \quad (7)$$

where M , N and Δx , Δy represent the resolution and the sampling interval of the hologram in horizontal and vertical directions, respectively. As the sampling interval is increased, the interval of the overlapped diffraction field in the hologram plane will be reduced according to Eq. (6). It results in the aliasing phenomenon appearing in the hologram plane, and occurring conditions of the aliasing are determined by:

$$\begin{aligned} \epsilon_x &< \frac{M \cdot \Delta x + M_1 \cdot \Delta x_1}{2}, \\ \epsilon_y &< \frac{N \cdot \Delta y + N_1 \cdot \Delta y_1}{2}. \end{aligned} \quad (8)$$

When the number of overlapped diffraction field in the hologram plane increased, the amplitude distribution can be smooth. However, the overlapped diffraction field will cause the structural noise contained in the phase-only hologram. An initial random phase should be added to the input image to smooth the diffraction field furthermore and to eliminate the noise. And in order to avoid strong interference among points, we need to consider the relationship between Airy disk diameter d_a and the sampling interval Δx_1 , the relation is given as follows:

$$\begin{aligned} d_a &= 2d_1 \tan\left(\frac{1.22\lambda}{\Delta x \cdot M}\right), \\ \Delta x_1 &> d_a. \end{aligned} \quad (9)$$

The sampling interval of the object Δx_1 should larger than d_a to avoid the strong speckle noise.

Except for the Eq. (9) limit the Δx_1 , the sampling interval Δx_1 also limited by the spatial bandwidth product of the SLM and the resolving power of the human eye, these relations are given by:

$$\Delta x_1 \cdot M < d_1 \tan[\sin^{-1}(\lambda/\Delta x)], \quad (10)$$

$$\Delta x_1 < d_o \frac{1.22\lambda}{D_e}. \quad (11)$$

where D_e represent the pupil diameter and d_o is the observer distance. In summary, the sampling interval of the object is limited by three reasons: (1) the diameter of the Airy disk, (2) the spatial bandwidth product of the SLM, (3) the resolving power of the human eye. By simultaneously solving the Eqs. (9), (10) and (11), we can obtain the limitations of M , which are expressed as:

$$\frac{d_1 D_e \tan[\sin^{-1}(\lambda/\Delta x)]}{1.22d_o\lambda} < M < \frac{\tan[\sin^{-1}(\lambda/\Delta x)]}{2 \tan(1.22\lambda/(\Delta x \cdot M))}. \quad (12)$$

The Eqs. (9), (11) and (12) indicate a way to choose the suitable parameters of the object to obtain an acceptable image quality in phase-only hologram reconstruction.

3.2 Holographic See-Through Display System

The designed holographic see-through display system is shown in Fig. 3. The input light source firstly passes through a collimating and beam expanding system. After the modulation of SLM, we set a barrier to filter the other-order light and only pass through the needed information. An ocular lens is set to enable virtual objects to be imaged in the retina and extend the system field of view (FOV), and a mirror and a beam splitter are set to mix the visual signals into real scenes. d_B represents the distance between SLM and barrier, d_{BO} represents the distance between the barrier and the ocular lens, and d_{OBS} represents the path length between the ocular lens and the beam splitter (BS).

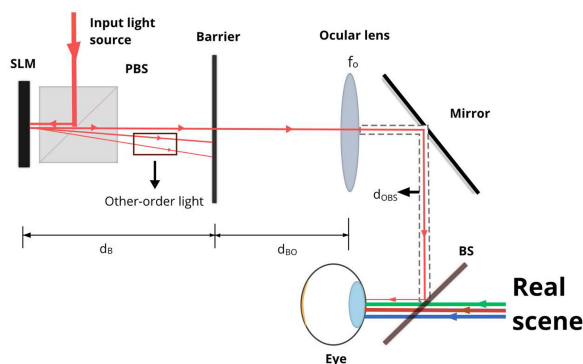


Fig. 3. Holographic see-through display system.

TABLE 1
Numerical Reconstruction Conditions

	Case1	Case2
CGH resolution $M \times N$	1920×1080	1920×1080
Object resolution $M1 \times N1$	3072×3072	3072×3072
CGH pixel pitch Δx	8.0 μm	8.0 μm
Object pixel pitch Δx_1	8.0 μm	8.0 μm
Wavelength λ	532.0 nm	532.0 nm
Diffraction distance d_1	0.50 m	0.50 m
Number of object slices n	256	256
Depth step Δz	3×0.104 mm	3×0.104 mm
Initial phase φ_i	uniform phase	random phase

4. Results

4.1 Numerical Simulation Results

The numerical reconstruction conditions of Fig. 4 are given in Table 1. Fig. 4(a) is the original image with depth information and Fig. 4(b) shows the amplitude distribution in the hologram plane. Figs. 4(c) and 4(d) show the reconstructed image from the phase-only hologram by removing the amplitude information without random phase and with random phase, respectively. We can see from Fig. 4(c) that directly remove the amplitude information will dramatic degrade the reconstructed image quality and the hologram is hard to recover the object which is larger than hologram plane. Although by adding a random phase to the original image can solve the problem, the speckle noise appears in the reconstructed image and degrades the image quality as shown in Fig. 4(d).

Figure 5 shows the numerical results with the proposed method, the main numerical conditions are given in Table 2. Figs. 5(a), 5(b) and 5(c) show the amplitude distribution in the hologram and the reconstructed image from the diffraction field and phase-only hologram, respectively. The resolution and the sampling interval of the object are 256×256 and $96.0 \mu\text{m}$, respectively. The size of the object is larger than the hologram. However, as we can see from Figs. 5(b), 5(c), the large part can recover from the hologram, and the quality of the reconstructed image from the phase-only hologram is nearly equal to the quality from complex amplitude. Fig. 5(d) shows the reconstructed image from the phase-only hologram with random phase. As shown in the red box in Figs. 5(b), 5(c) and 5(d), because the sampling interval is enlarged, the interference among points are weak and compared with Fig. 4(d) the influence of the speckle noise is reduced.

Figures 5(e) and 5(f) show the reconstructed result at $\Delta x_1 = 96.0 \mu\text{m}$ and $\Delta x_1 = 40.0 \mu\text{m}$ when defocus the reconstructed image, respectively. The overlapped reconstructed image phenomenon in Fig. 5(f) is replaced by the blurred image shown in Fig. 5(e) when increasing the sampling

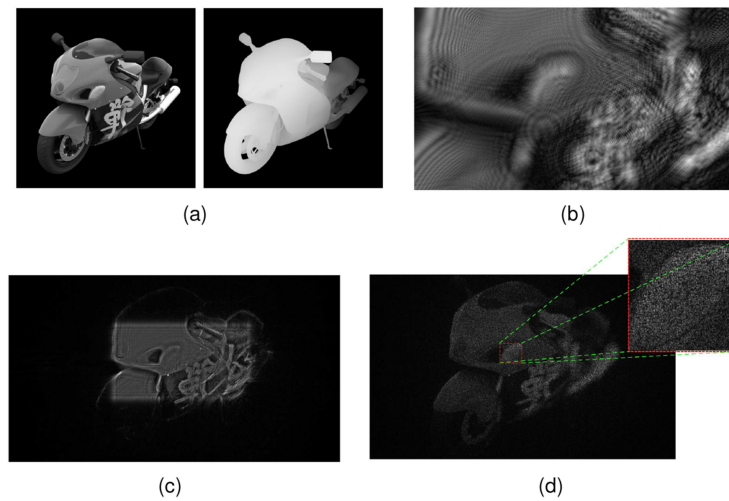


Fig. 4. Numerical results: (a) original image with depth channel, (b) diffraction field in hologram plane; (c) reconstructed image from phase-only hologram without random phase, and (d) with random phase.

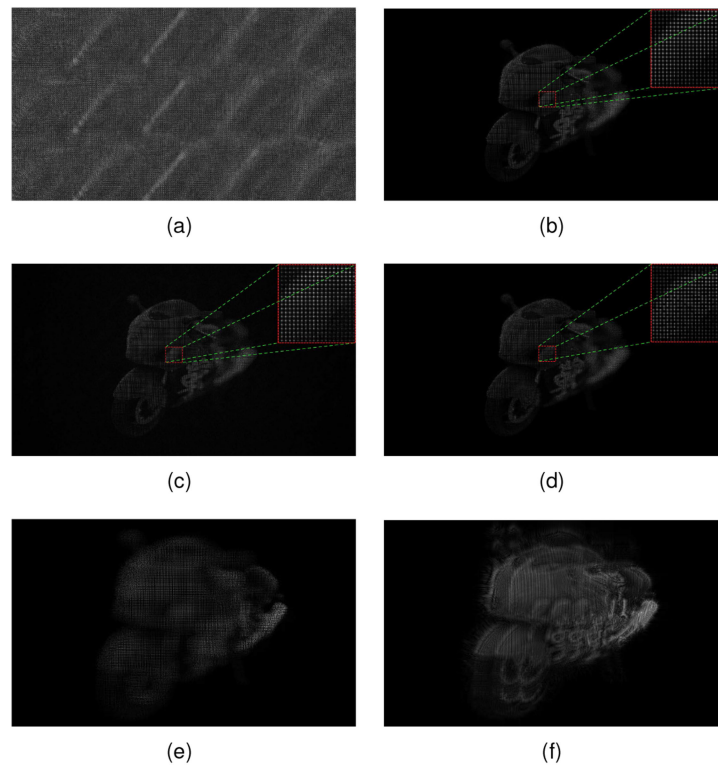


Fig. 5. Numerical results of the proposed method: (a) diffraction field in hologram plane, (b) reconstructed image from complex amplitude, (c) phase-only hologram, and (d) phase-only hologram with random phase; (e) defocus the reconstructed image at $\Delta x_1 = 96.0 \mu\text{m}$, (f) $\Delta x_1 = 40.0 \mu\text{m}$.

interval of the object. The overlapped reconstructed image phenomenon [30]–[32] can be solved with the proposed method, when the number of the diffraction field increased in the hologram, the overlapped image will be replaced by the blurred image, which is more acceptable by the human eye.

TABLE 2
Numerical Reconstruction Conditions

CGH resolution $M \times N$	1920 × 1080
Object resolution $M1 \times N1$	256 × 256
CGH pixel pitch Δx	8.0 μm
Object pixel pitch Δx_1	12 × 8.0 μm
Wavelength λ	532.0 nm
Diffraction distance d_1	0.50 m
Number of object slices n	256
Depth step Δz	3 × 0.104 mm

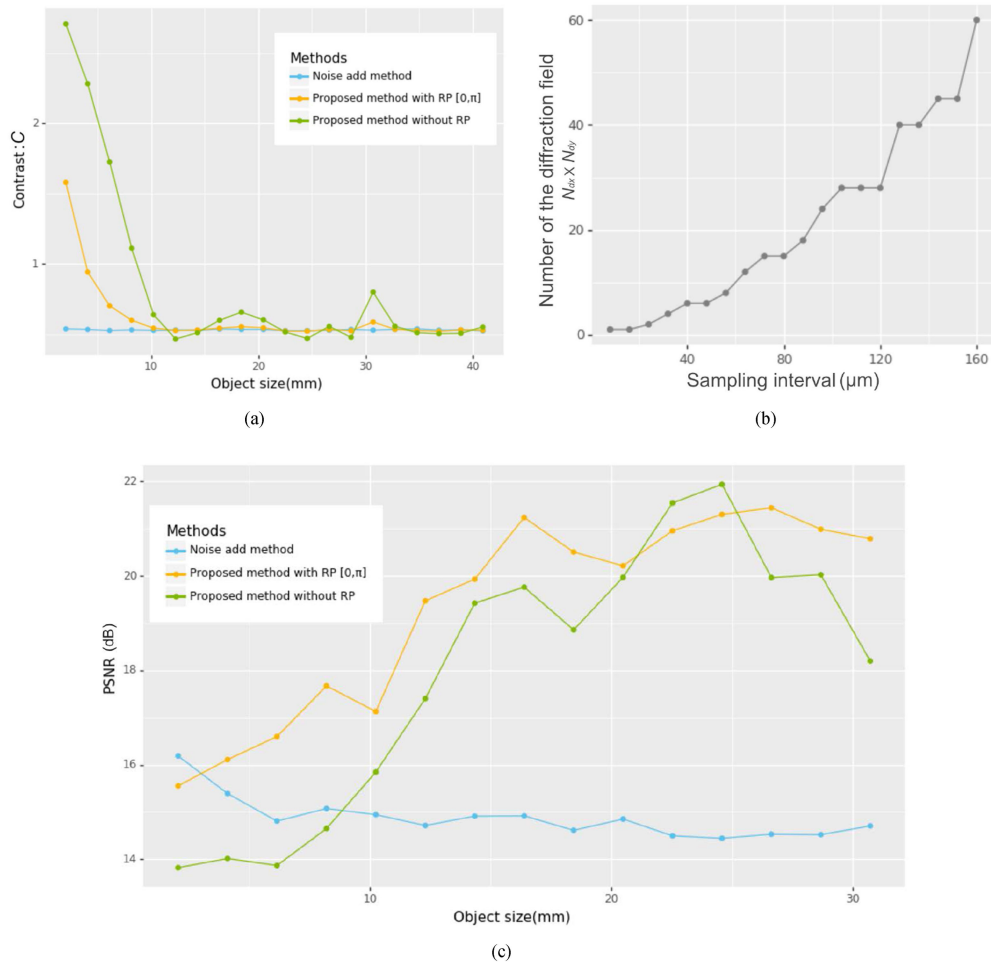


Fig. 6. Numerical result: (a) relationship between the object size and contrast, (b) the sampling interval and number of the overlapped diffraction field, and (c) the object size and reconstructed image quality.

In order to measure the effect of the lost amplitude information in the phase-only hologram, the contrast C is used to represent the amplitude uniformity in the hologram plane, lower value means the much less information lost, and the expression is defined by:

$$C = \frac{\sigma}{\mu}, \quad (13)$$

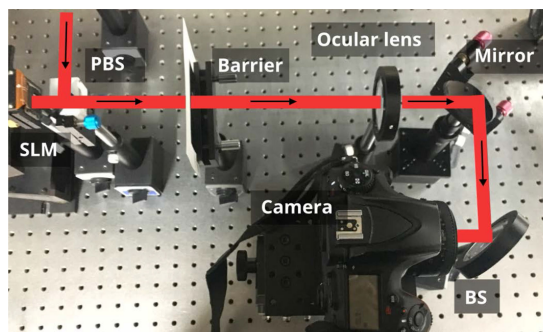


Fig. 7. Optical experiment system.

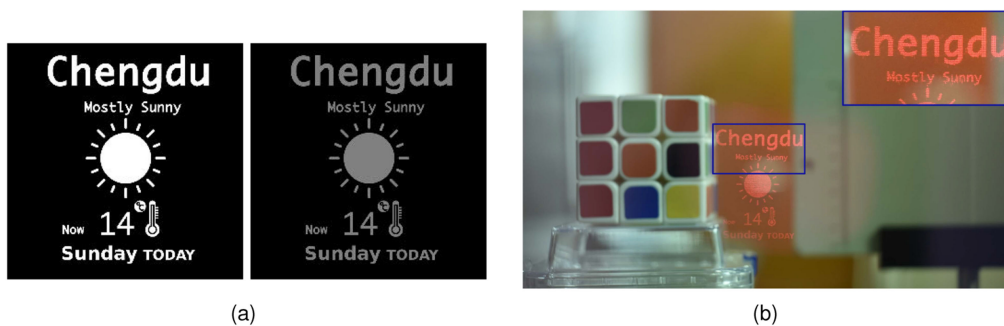


Fig. 8. Optical results: (a) input image1 with depth channel, (b) camera focused on the image1.

where σ and μ are the standard deviation and the mean value of the amplitude distribution in the hologram plane, respectively. We use Fig. 4(a) with constant depth information as input object and the resolution is 256×256 , the diffraction distance is set to $d_1 = 0.5$ m. For the purpose of test the image quality of the reconstructed image, we resampling the reconstructed image to the resolution of 256×256 , and we use the PSNR (Peak signal-to-noise ratio) to measure the reconstructed image quality.

Figure 6(a) shows the relationship between object size and the contrast of the diffraction field in the hologram plane, Fig. 6(b) shows the relationship between the sampling interval and the number of the diffraction field and Fig. 6(c) shows the relationship between object size and image quality. As shown in Figs. 6(a) and 6(b), the proposed method can reduce the contrast in the hologram plane and the increase the recorded information of the object in the phase-only hologram. In Fig. 6(c), we can see the reconstructed image quality of the proposed method is increased by enlarging the sampling interval, and the quality of the proposed method is better than that of the random phase method [20]. Moreover, as the size of the object is increased, the calculation time of the random phase method is increased, and the PSNR of the reconstructed is nearly unchanged. Compared with the random phase method, the proposed method gains unchanged and shorter calculation time but the better reconstructed image quality when the size of the object increases.

4.2 Optical Experiment Results

The optical experiment system is shown in Fig. 7, The resolution and the pixel pitch of the SLM are 3840×2160 and $3.74 \mu\text{m}$, respectively. We use a red laser with 671.0 nm wavelength as input light source. The d_B , d_{B0} and d_{OBS} are set to 17.0 cm, 17.0 cm, and 8.0 cm, respectively. And the focal length of the ocular lens is 150.0 mm. We use a camera (Nikon D810 with a 50.0 mm lens) to capture the image.

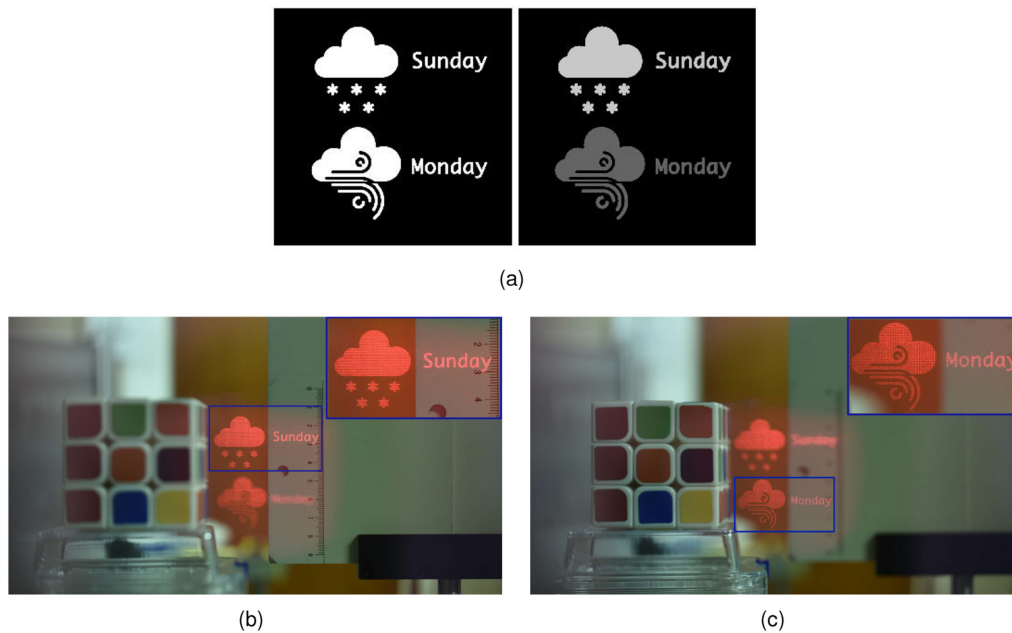


Fig. 9. Optical results: (a) input image2 with depth channel, (b) camera focused on “Sunday” and (c) focused on “Monday” (see Visualization1).

Figure 8 shows the display results with the proposed method. Fig. 8(a) shows the input image1 with depth channel. The resolution of the images are 256×256 , and the sampling interval of the input images are set to $24 \times 3.74 \mu\text{m}$. And the diffraction distance is set to 0.20 m. Because of the influences of the ocular lens, the reconstructed image is larger than the physical size of the original image, and the focus distance is also changed. Fig. 8(b) shows the captured image when the camera focus at 0.50 m. Fig. 9 shows the reconstructed result when the camera focus on the different plane, Fig. 9(a) shows the input image2 with depth channel. Figs. 9(b) and 9(c) show the captured images when the camera focused at 0.68 m and 0.49 m, respectively.

5. Conclusion

In this study, we have analyzed the reason of aliasing which is the overlapped diffraction field phenomenon in the point-based method firstly. Then, we take advantage of this phenomenon and propose a simple method based on aliasing reuse to enhance the reconstructed image quality. Moreover, we have indicated a way to choose the suitable parameters of the object by analyzing the relationship between the sampling interval and the image quality. Based on this method, the speckle noise and the amplitude information loss problem can be improved, and the calculated time is reduced at the same time. In addition, we have designed a holographic see-through display system to demonstrate the effectiveness of the proposed method. We believe that our method has potential applications in the field of AR.

References

- [1] R. Azuma, Y. Baillet, R. Behringer, S. Feiner, S. Julier, and B. MacIntyre, “Recent advances in augmented reality,” *IEEE Comput. Graph. Appl.*, vol. 21, no. 6, pp. 34–47, Nov./Dec. 2001.
- [2] J. Carmigniani, B. Furht, M. Anisetti, P. Ceravolo, E. Damiani, and M. Ivkovic, “Augmented reality technologies, systems and applications,” *Multimedia Tools Appl.*, vol. 51, no. 1, pp. 341–377, 2011.
- [3] I. Rabbi and S. Ullah, “A survey on augmented reality challenges and tracking,” *Acta Graphica*, vol. 24, no. 1–2, pp. 29–46, 2013.

- [4] S. Yano, S. Ide, T. Mitsuhashi, and H. Thwaites, "A study of visual fatigue and visual comfort for 3D HDTV/HDTV images," *Displays*, vol. 23, no. 4, pp. 191–201, 2002.
- [5] S. J. Watt, K. Akeley, M. O. Ernst, and M. S. Banks, "Focus cues affect perceived depth," *J. Vis.*, vol. 5, no. 10, pp. 7–7, 2005.
- [6] D. M. Hoffman, A. R. Girshick, K. Akeley, and M. S. Banks, "Vergence–accommodation conflicts hinder visual performance and cause visual fatigue," *J. Vis.*, vol. 8, no. 3, pp. 33–33, 2008.
- [7] J. Han, J. Liu, X. Yao, and Y. Wang, "Portable waveguide display system with a large field of view by integrating freeform elements and volume holograms," *Opt. Exp.*, vol. 23, no. 3, pp. 3534–3549, 2015.
- [8] E. Moon, M. Kim, J. Roh, H. Kim, and J. Hahn, "Holographic head-mounted display with RGB light emitting diode light source," *Opt. Exp.*, vol. 22, no. 6, pp. 6526–6534, 2014.
- [9] G. Li, D. Lee, Y. Jeong, J. Cho, and B. Lee, "Holographic display for see-through augmented reality using mirror-lens holographic optical element," *Opt. Lett.*, vol. 41, no. 11, pp. 2486–2489, 2016.
- [10] P. Sun, S. Chang, S. Liu, X. Tao, C. Wang, and Z. Zheng, "Holographic near-eye display system based on double-convergence light Gerchberg–Saxton algorithm," *Opt. Exp.*, vol. 26, no. 8, pp. 10140–10151, 2018.
- [11] J.-S. Chen and D. Chu, "Improved layer-based method for rapid hologram generation and real-time interactive holographic display applications," *Opt. Exp.*, vol. 23, no. 14, pp. 18143–18155, 2015.
- [12] Y. Zhao, L. Cao, H. Zhang, D. Kong, and G. Jin, "Accurate calculation of computer-generated holograms using angular-spectrum layer-oriented method," *Opt. Exp.*, vol. 23, no. 20, pp. 25440–25449, 2015.
- [13] P. Tsang, T.-C. Poon, and Y. Wu, "Review of fast methods for point-based computer-generated holography," *Photon. Res.*, vol. 6, no. 9, pp. 837–846, 2018.
- [14] T. Shimobaba, T. Kakue, and T. Ito, "Review of fast algorithms and hardware implementations on computer holography," *IEEE Trans. Ind. Inform.*, vol. 12, no. 4, pp. 1611–1622, Aug. 2016.
- [15] M. E. Lucente, "Interactive computation of holograms using a look-up table," *J. Electron. Imag.*, vol. 2, no. 1, pp. 28–35, 1993.
- [16] S.-C. Kim and E.-S. Kim, "Effective generation of digital holograms of three-dimensional objects using a novel look-up table method," *Appl. Opt.*, vol. 47, no. 19, pp. D55–D62, 2008.
- [17] S.-C. Kim, J.-M. Kim, and E.-S. Kim, "Effective memory reduction of the novel look-up table with one-dimensional sub-principle fringe patterns in computer-generated holograms," *Opt. Exp.*, vol. 20, no. 11, pp. 12021–12034, 2012.
- [18] J. Jia *et al.*, "Reducing the memory usage for effective computer-generated hologram calculation using compressed look-up table in full-color holographic display," *Appl. Opt.*, vol. 52, no. 7, pp. 1404–1412, 2013.
- [19] S. Jiao, Z. Zhuang, and W. Zou, "Fast computer generated hologram calculation with a mini look-up table incorporated with radial symmetric interpolation," *Opt. Exp.*, vol. 25, no. 1, pp. 112–123, 2017.
- [20] A. W. Lohmann and D. Paris, "Binary Fraunhofer holograms, generated by computer," *Appl. Opt.*, vol. 6, no. 10, pp. 1739–1748, 1967.
- [21] M. Makowski, M. Sypek, A. Kolodziejczyk, and G. Mikula, "Three-plane phase-only computer hologram generated with iterative Fresnel algorithm," *Opt. Eng.*, vol. 44, no. 12, 2005, Art. no. 125805.
- [22] J. R. Fienup, "Reconstruction of an object from the modulus of its Fourier transform," *Opt. Lett.*, vol. 3, no. 1, pp. 27–29, 1978.
- [23] Y. Takaki and M. Yokouchi, "Speckle-free and grayscale hologram reconstruction using time-multiplexing technique," *Opt. Exp.*, vol. 19, no. 8, pp. 7567–7579, 2011.
- [24] S.-J. Liu, D. Wang, and Q.-H. Wang, "Speckle noise suppression method in holographic display using time multiplexing technique," *Opt. Commun.*, vol. 436, pp. 253–257, 2019.
- [25] J. Amako, H. Miura, and T. Sonehara, "Speckle-noise reduction on kinoform reconstruction using a phase-only spatial light modulator," *Appl. Opt.*, vol. 34, no. 17, pp. 3165–3171, 1995.
- [26] R. Eschbach, "Comparison of error diffusion methods for computer-generated holograms," *Appl. Opt.*, vol. 30, no. 26, pp. 3702–3710, 1991.
- [27] P. W. M. Tsang and T.-C. Poon, "Novel method for converting digital Fresnel hologram to phase-only hologram based on bidirectional error diffusion," *Opt. Exp.*, vol. 21, no. 20, pp. 23680–23686, 2013.
- [28] P. W. M. Tsang, Y.-T. Chow, and T.-C. Poon, "Generation of phase-only Fresnel hologram based on down-sampling," *Opt. Exp.*, vol. 22, no. 21, pp. 25208–25214, 2014.
- [29] T. Shimobaba, T. Kakue, N. Okada, M. Oikawa, Y. Yamaguchi, and T. Ito, "Aliasing-reduced Fresnel diffraction with scale and shift operations," *J. Opt.*, vol. 15, no. 7, 2013, Art. no. 075405.
- [30] X.-B. Dong, S.-C. Kim, and E.-S. Kim, "Mpeg-based novel look-up table for rapid generation of video holograms of fast-moving three-dimensional objects," *Opt. Exp.*, vol. 22, no. 7, pp. 8047–8067, 2014.
- [31] S.-C. Kim, X.-B. Dong, M.-W. Kwon, and E.-S. Kim, "Fast generation of video holograms of three-dimensional moving objects using a motion compensation-based novel look-up table," *Opt. Exp.*, vol. 21, no. 9, pp. 11568–11584, 2013.
- [32] X.-B. Dong, S.-C. Kim, and E.-S. Kim, "Three-directional motion compensation-based novel-look-up-table for video hologram generation of three-dimensional objects freely maneuvering in space," *Opt. Exp.*, vol. 22, no. 14, pp. 16925–16944, 2014.
- [33] T. Shimobaba *et al.*, "Random phase-free kinoform for large objects," *Opt. Exp.*, vol. 23, no. 13, pp. 17269–17274, 2015.
- [34] M. Makowski, "Minimized speckle noise in lens-less holographic projection by pixel separation," *Opt. Exp.*, vol. 21, no. 24, pp. 29 205–29 216, 2013.
- [35] C. Chang, J. Xia, L. Yang, W. Lei, Z. Yang, and J. Chen, "Speckle-suppressed phase-only holographic three-dimensional display based on double-constraint Gerchberg–Saxton algorithm," *Appl. Opt.*, vol. 54, no. 23, pp. 6994–7001, 2015.
- [36] Y. Qi, C. Chang, and J. Xia, "Speckleless holographic display by complex modulation based on double-phase method," *Opt. Exp.*, vol. 24, no. 26, pp. 30368–30378, 2016.